Journal of Organometallic Chemistry 695 (2010) 1002–1005

Contents lists available at ScienceDirect

Journal of Organometallic Chemistry

journal homepage: www.elsevier.com/locate/jorganchem

A new low temperature methodology to obtain pure nanocrystalline nickel borate

Menaka [a], Samuel E. Lofland [b], Kandalam V. Ramanujachary [c], Ashok K. Ganguli [a,*]

[a] Department of Chemistry, Indian Institute of Technology Delhi, Hauz Khas, New Delhi 110016, India
[b] Department of Physics and Astronomy, Rowan University, Glassboro, NJ 08028, USA
[c] Department of Chemistry and Biochemistry, Rowan University, Glassboro, NJ 08028, USA

ARTICLE INFO

Article history:
Received 30 September 2009
Received in revised form 19 October 2009
Accepted 20 October 2009
Available online 26 October 2009

Keywords:
Borate
Nanostructure
Reverse micelle

ABSTRACT

The present study focuses on the development of a new route for the synthesis of pure nickel borate nanoparticles using reverse micellar route. Nickel borate nanoparticles (25 nm) were synthesized from a precursor (obtained by reverse micellar route) containing both nickel and boron (nickel nitrate and sodium borohydride as starting materials). Decomposition of the precursor at a temperature of ~800 °C yielded pure nickel borate nanoparticles. This was confirmed by powder X-ray diffraction and transmission electron microscopy. These nanoparticles show an antiferromagnetic ordering with Néel temperature of 47 K.

1. Introduction

Metal borates are of considerable interest because of several applications. Borates are stable at high temperature and have high luminescence which has applications in lasers, optical glasses and phosphors [1]. Structurally, borates are analogous to silicates except for the modes of coordination. Silicates are coordinated to oxygen in a tetrahedral geometry while borates can coordinate to oxygen both in triangular and tetrahedral geometry. However, it is still not easy to predict which coordination of boron will dominate in a structure at ambient conditions. In the rare earth borate like $REBO_3$ (*RE* = Pr, Nd, Sm-Dy, Yb), a trigonal coordinate of boron is stabilized at high pressure [2–3]. It is known that by increase in pressure, the higher coordination of boron in borates would be stable [4]. Borates prefer corner sharing of the triangular (BO_3) or tetrahedral (BO_4) polyhedra over a face or edge-sharing to form a rigid network and these networks can have high thermal stability [5]. Among the known borates, nickel orthoborate (isomorphous with magnesium orthoborate) [6] exhibits magnetic, catalytic and phosphorescent properties [7–9]. The detailed structural aspects of nickel borate have been studied by Gòtz et al. and Pardo et al. [6,10]. It has been found that nickel orthoborate crystallizes in the kotoite structure with an orthorhombic cell [10,11]. The orthoborates have discrete trigonal BO_3 polyhedra in their lattice. Nickel borates have two types of Ni atoms, both octahedrally coordinated and linked together by O sharing to form a three-dimensional network. Each O atom is surrounded by three Ni atoms and one B atom arranged in an irregular tetrahedron as shown in Fig. 1.

The synthesis of nickel borate has earlier been carried out by the solid state route at high temperature [11]. The present study discusses a new low temperature method to produce a nanocrystalline form of nickel borate. To the best of our knowledge there is no report on nanostructured nickel borates although various morphologies of zinc, copper and magnesium borates have been reported [12–15]. The present study emphasizes the control of the size of nickel borates nanoparticles via microemulsion route for the first time and we have also investigated the magnetic property of nickel orthoborate.

2. Experimental

Commercially available cetyltrimethylammonium bromide (CTAB, spectrochem, 99%), nickel nitrate hexahydrate (BDH 97%), sodium borohydride (spectrochem, 98%), 1-butanol (Qualigens, 99.5%), isooctane (spectrochem, 99%), chloroform (SRL, 99.5%), ethanol (Merck, 99.9%) and methanol (Qualigens, 99%) were used in the synthesis. Two microemulsions consisting of CTAB as surfactant, 1-butanol as cosurfactant, isooctane as hydrocarbon phase and the aqueous phase were prepared. The composition of the microemulsion was taken in the following weight fractions: 16.94% of CTAB, 13.99% of *n*-butanol, 58.94% of isooctane and 10.12% of the aqueous phase. About 0.1 M metal nitrate (Ni^{2+}) solution was used as the aqueous phase in one microemulsion whereas 0.3 M sodium borohydride solution was used in the second microemulsion. The reaction was accomplished by mixing the two microemulsions and stirred overnight at room temperature. Imme-

* Corresponding author. Tel.: +91 11 26591511; fax: +91 11 26854715.
E-mail address: ashok@chemistry.iitd.ernet.in (A.K. Ganguli).

0022-328X/$ - see front matter © 2009 Elsevier B.V. All rights reserved.
doi:10.1016/j.jorganchem.2009.10.023

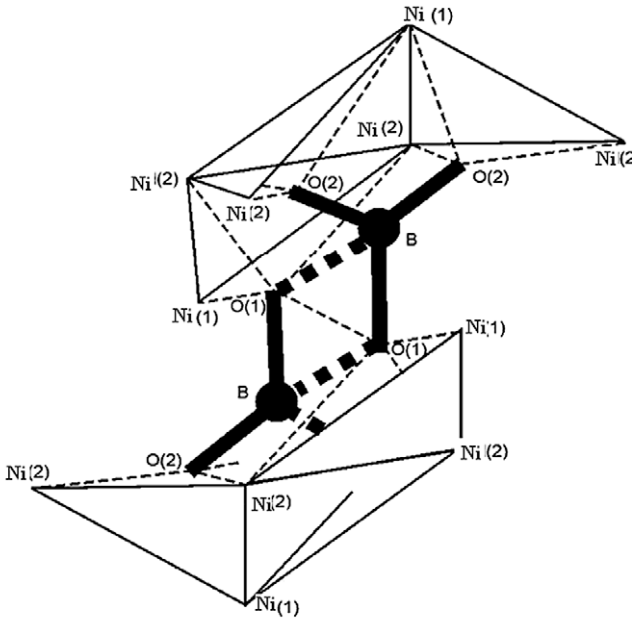

Fig. 1. Structure of nickel orthoborate $Ni_3(BO_3)_2$.

diately after mixing a black precipitate was observed with the evolution of H_2 gas. After an hour the black precipitate gets converted to a green one due to the presence of nickel borate ions at room temperature. The green colored precipitate formed was separated from the apolar solvent by centrifugation and washed with 1:1 mixture of $CHCl_3$ and CH_3OH. The precipitate was dried at room temperature and heated at 800 °C in air to obtain the parrot green nickel borate nanoparticles [16–18].

PXRD studies were carried out on a Bruker D-8 Advance X-ray diffractometer using Ni filtered Cu Kα radiation. Normal scans were recorded with a 2θ step of 0.02° and a residence time of 1 s. With the help of X-ray line broadening studies, the crystallite size could be obtained for the borate particles. IR spectra were recorded on disks obtained after mixing with KBr and loaded on a Nicolet Protege 460 (FTIR) spectrometer operating in the range of 400–4000 cm^{-1}. TEM was recorded on a Technai G^2 20 (FEI) electron microscope operated at 200 kV. TEM specimens were prepared by loading a drop of the ultrasonically dispersed sample in ethanol on a carbon-coated copper grid and dried in air. Magnetization studies of the metal borate was measured at temperatures ranging from 5 to 300 K, in applied fields of up to 10 kOe with a Quantum Design physical properties measurement system (see Fig. 2).

3. Results and discussion

Nickel borate has been prepared earlier by solid state route at high temperature (~1200 °C) [11]. The aim of this study was to develop low temperature routes for the synthesis of nickel borate and to control the particles size to finally obtain nanocrystalline nickel borate particle. To prepare nanocrystalline nickel borate first a nickel–boron precursor was synthesized using the reverse micellar route. It is known that sodium borohydride acts as a reducing agent and during the process leads to the production of H_2 which can further reduce metal ions like Ni^{2+} as shown in Eqs. (1) and (2) [19,20]

Table 1
FTIR spectrum of nickel–boron precursor obtained at room temperature.

Frequency (cm^{-1})	Assignment	Description
3436.68 (bs*)	ν(O–H str.)	Observed due to presence of water molecules [21]
1639.41 (w*)	δ(H–O–H)	Observed due to presence of water molecules [21]
1385.18 (s*)	δ(B–O–H)	Unique to $NaBO_2$ [21]
985.05 (s*)	ν(O–$B_{(4)}$)	B–O stretching [21]
696.61 (m*)	γ(O–$B_{(4)}$)	Unique to $NaBO_2$ [21]
415.51 (w*)	δ(B–O)	B–O bending [21]

* *Abbreviation of the symbols:* s, strong; b, broad; w, weak; bs, broad and strong; m, medium; bw, broad and weak; ss, sharp and strong.

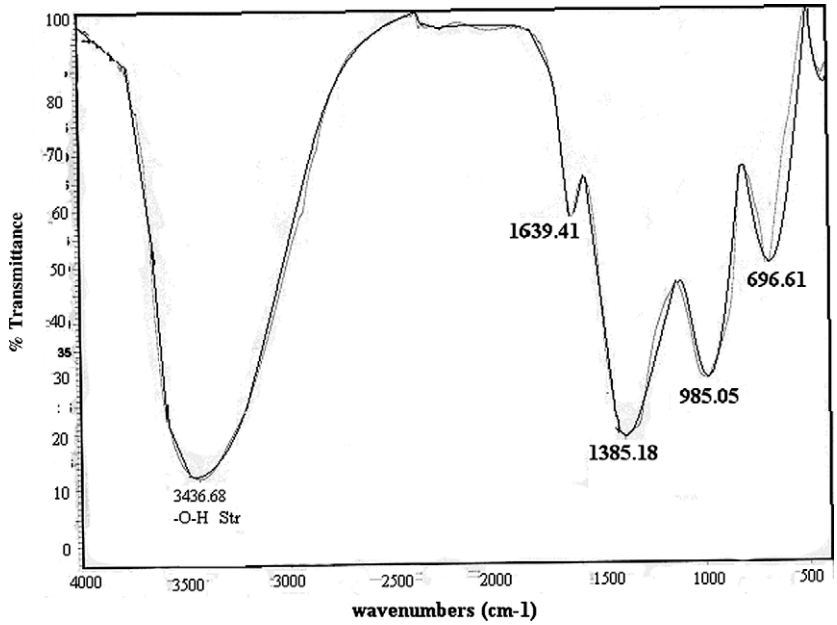

Fig. 2. FTIR spectrum of nickel–boron precursor obtained at room temperature by reverse micellar route.

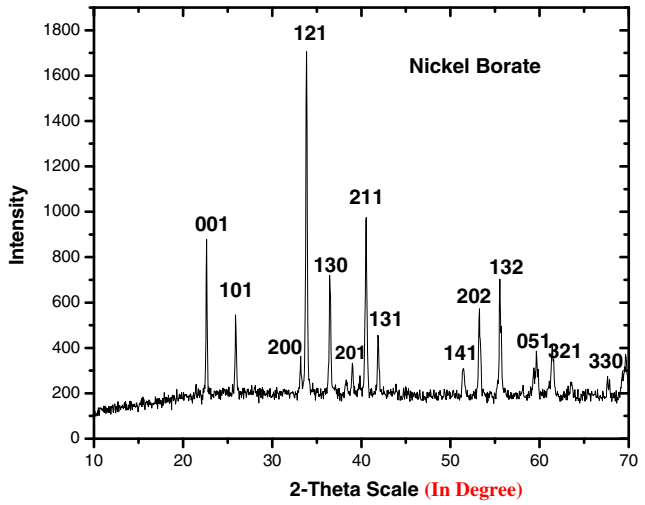

Fig. 3. PXRD pattern of pure nickel borate $Ni_3(BO_3)_2$ obtained by heating the nickel boron precursors at 800 °C in air.

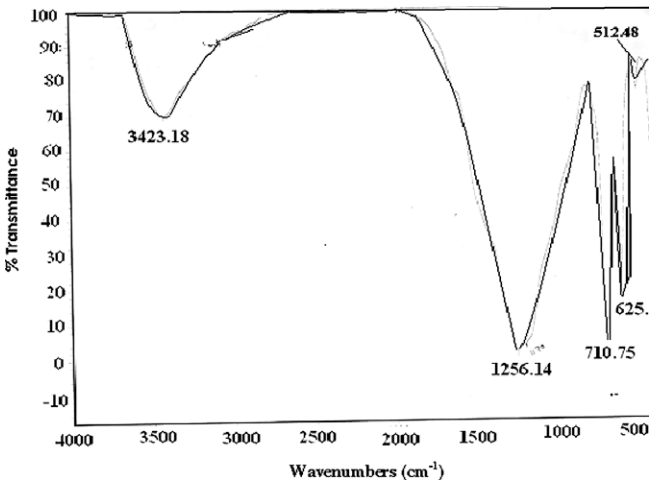

Fig. 5. FTIR spectrum of nickel borate $Ni_3(BO_3)_2$ obtained by heating the nickel–boron precursor at 800 °C in air.

$$NaBH_4 + 2H_2O \rightarrow NaBO_2 + 4H_2 \quad (1)$$

$$Ni^{2+} + 4H_2 \overset{\text{Room temperature}}{\rightarrow} Ni \quad (2)$$

$$Ni \overset{\text{Hydrolysis in } H_2O}{\rightarrow} NiO \cdot XH_2O \quad (3)$$

Further hydrolysis of nickel metal leads to the formation of hydrated nickel oxide as shown in Eq. (3). Based on the above reactions, nickel boron precursor would be composed of a homogeneous mixture of nickel oxide and hydrated sodium metaborate $NaBO_2$. The above has been deduced by FTIR studies which shows the presence of BO_2^- (metaborate) ions and the hydrated species (O–H stretching) [21]. The details of the vibrational modes are given in Table 1. The powder X-ray diffraction (PXRD) pattern shows that the nickel–boron precursor obtained at room temperature using the reverse micellar method is amorphous in nature. Decomposition of the above precursor in air at 800 °C led to the formation of a parrot green product whose powder X-ray diffraction (PXRD) pattern was satisfactorily indexed on the basis of an orthorhombic cell as reported for nickel borate ($Ni_3(BO_3)_2$) (JCPDS No. 75-1809) (Fig. 3). The average crystallite size was evaluated from X-ray line broadening studies (using Scherrer's equation) and was found to be ~30 nm. The crystallite size obtained from line broadening studies is in closed agreement with transmission electron microscopic studies which shows nanoparticles of 25 nm size. These nanoparticles are spherical and uniformly distributed (Fig. 4). The presence of BO_3^{3-} (orthoborate) ions in nickel borate $Ni_3(BO_3)_2$ have also been shown by the typical FTIR spectrum (Fig. 5). The details of each band have been given in Table 2. The magnetic properties of the nickel borate $Ni_3(BO_3)_2$, shows an antiferromagnetic behavior with a Néel temperature of 47 K (Fig. 6). The effective magnetic moment was calculated to be 3.08 BM per mole of Ni from the high temperature data of the inverse susceptibility plot (inset of (Fig. 6)). The observed moment is in close agreement with that expected for free Ni(II)-ion.

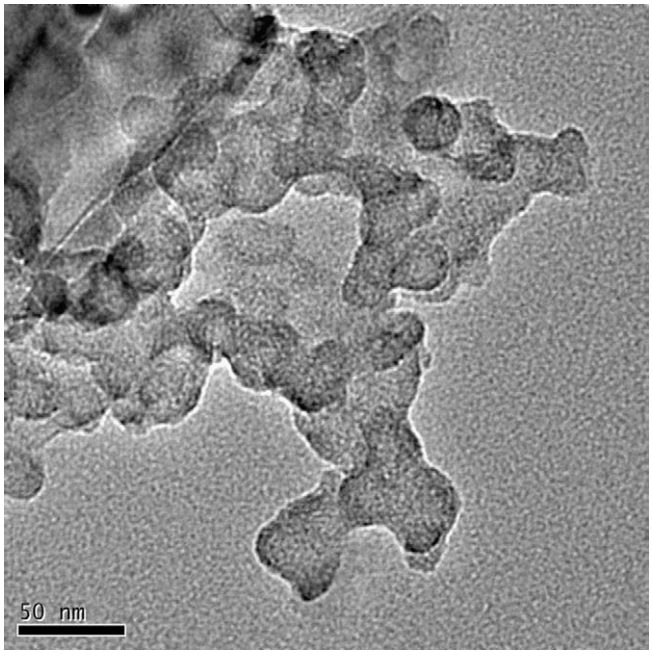

Fig. 4. TEM micrograph of nickel borate $Ni_3(BO_3)_2$ obtained by heating the nickel–boron precursor at 800 °C in air.

Table 2
FTIR spectrum of nickel borate obtained at 800 °C.

Frequency (cm^{-1})	Assignment	Description
3423.18 (bw*)	–O–H stretching	Absorbed water molecule
1256.14 (s*)	ν3 –B–O stretching	Asymmetric –BO stretching present in triangular borate $BO3^{3-}$ (broad and strong)
710.75 (ss*)	ν2 –B–O bending	Out-of-plane bending, sharp and strong
625.34 (m*)	ν4 –B–O bending	In-plane bending, medium

* *Abbreviation of the symbols:* s, strong; b, broad; w, weak; bs, broad and strong; m, medium; bw, broad and weak; ss, sharp and strong.

4. Conclusions

Nickel borate ($Ni_3(BO_3)_2$) nanoparticles were successfully prepared by thermal decomposition (at 800 °C) of nickel–boron precursor (obtained via the reverse micellar route). Monophasic and uniform spherical nanoparticles of nickel borate of 25 nm size were obtained for the first time. Earlier synthesis of nickel borate was possible at high temperature of ~1200 °C. This new methodology allows us to obtain pure phase at much lower temperature and

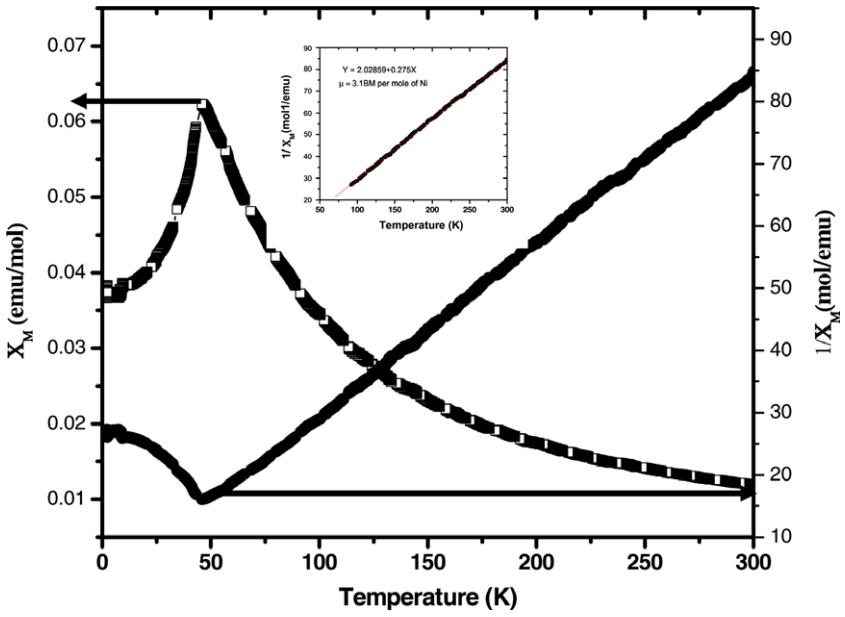

Fig. 6. Plot of the magnetic susceptibility and inverse of magnetic susceptibility (in an inset) with temperature of nickel borate $Ni_3(BO_3)_2$ obtained by heating the nickel–boron precursor at 800 °C in air.

the particles are 20–30 nm in size. Magnetization data shows an antiferromagnetic behavior with a Nèel temperature of 47 K.

Acknowledgment

A.K.G. thanks the NSTI, Department of Science and Technology, and CSIR, Government of India, for financial support. Menaka thanks UGC, Government of India for a fellowship.

References

[1] Y. Zhang, J.K. Liang, X.L. Chen, M. He, T. Xu, J. Alloys Compd. 327 (2001) 96.
[2] (a) H.J. Meyer, Naturwissenschaften 56 (1969) 458;
(b) H. J Meyer, A. Skokan, Naturwissenschaften 58 (1971) 566;
(c) H.J. Meyer, Naturwissenschaften 59 (1972) 215.
[3] H. Huppertz, B. von der Eltz, J. Am. Chem. Soc. 124 (2002) 9376.
[4] H. Emme, H. Huppertz, Chemistry (2003) 3623.
[5] S.K. Filatov, R.S. Bubnova, Phys. Chem. Glasses 41 (2000) 216.
[6] W. Gòtz, Naturwissenschaften 50 (1963) 567.
[7] J.P. Attfield, A.M.T. Bell, L.M. Rodrıguez-Martınez, J.M. Greneche, R. Retoux, M. Leblanc, R.J. Cernık, J.F. Clarke, D.A. Perkıns, J. Mater. Chem. 9 (1999) 205.
[8] R. Wolfe, R.D. Pıerce, M. Eıbschut, J.W. Nıelsen, Solid State Commun. 7 (1969) 949.
[9] A. Zletz (Amoco Corp.), US Patent Application 709, 790, 11 March 1985.
[10] J. Pardo, M. Martinez-Ripoll, S. Blanco-Garcia, Acta Crystallogr. B30 (1974) 37.
[11] H. Effenberger, F. Perttlik, Z. Kristallogr. 66 (1984) 129.
[12] E.M. Elssfah, A. Elsanousi, J. Zhang, H.S. Song, C. Tang, Mater. Lett. 61 (2007) 4358.
[13] Y. Zheng, Z. Wang, Y. Tian, Y. Qu, S. Li, D. An, X. Chen, S. Guan, Colloids Surf., A: Physicochem. Eng. Aspects 349 (2009) 156.
[14] C. Ting, D. Jian-Cheng, W. Long-Shuo, F. Gang, J. Mater. Process. Technol. 209 (2009) 4076.
[15] C. Ting, D. Jian-Cheng, W. Long-Shuo, Y. Fan, F. Gang, Mater. Lett. 62 (2008) 2057.
[16] T. Ahmad, K.V. Ramanujachary, S.E. Lofland, A.K. Ganguli, Solid State Sci. 8 (2006) 425.
[17] T. Ahmad, S. Vaidya, N. Sarkar, S. Ghosh, A.K. Ganguli, Nanotechnology 17 (2005) 1236.
[18] T. Ahmad, K.V. Ramanujachary, S.E. Lofland, A.K. Ganguli, J. Mater. Chem. 14 (2004) 3406.
[19] J.C. Walter, A. Zurawski, D. Montgomery, M. Thornburg, S. Revankar, J. Power Sources 179 (2008) 335.
[20] Y. Hou, H. Kondoh, T. Oht, S. Gao, Appl. Surf. Sci. 241 (2005) 218.
[21] L. Jun, X. Shuping, G. Shiyang, Spectrochim. Acta 51A (4) (1995) 519.